

Role of refractive index gradient in spin Hall effect of light

Hailu Luo, Shuangchun Wen,* Weixing Shu, and Dianyuan Fan

*Key Laboratory for Micro/Nano Opto-Electronic Devices of Ministry of Education,
School of Information Science and Engineering, Hunan University, Changsha 410082, People's Republic of China*
(Dated: March 22, 2019)

In this paper, we try to identify the role of refractive index gradient in spin Hall effect (SHE) of light from the viewpoint of classical electrodynamics. We demonstrate that the refractive index gradient can enhance or suppress the spin-to-orbital angular momentum conversion, and thus can control the SHE of light. Under the limit of ultra-large refractive index gradient, the polarization-dependent transverse shift is found to tend to a saturation value. The transverse shift is governed by the spin-to-orbital angular momentum conversion, clearly clarifying the role of refractive index gradient in the SHE. We suggest that the metamaterial whose refractive index can be tailored arbitrarily may become a viable candidate for amplifying or attenuating the SHE of light, and by properly facilitating the spin-to-orbital angular momentum conversion the SHE may be enhanced dramatically. These findings pave a pathway for modulating the SHE of light and can be extrapolated to other physical systems.

PACS numbers: 42.25.-p, 42.79.-e, 41.20.Jb

I. INTRODUCTION

The development of spin photonics has taken an important step forwards due to the recently experimental verifications of the spin Hall effect (SHE) of light [1, 2]. The SHE is a transport phenomenon, in which an applied field on the spin particles leads to a spin-dependent shift perpendicular to the electric field [3–5]. The SHE of light can be regarded as a direct optical analogy in which the spin electrons and electric potential are replaced by spin photons and refractive index gradient. The SHE of light sometimes referred to as the Fedorov–Imbert effect, was predicted theoretically by Fedorov [6], and was experimentally confirmed by Imbert [7]. The theory was extended in a formulation which shows that the transverse spatial separation of the left and right circularly polarized components on oblique incidence directly from the total angular momentum conservation [8, 9]. More recently, the interesting effect has also been observed in scattering from dielectric spheres [10], on the direction making an angle with the propagation axis [11], and in silicon via free-carrier absorption [12].

The polarization-dependent transverse shift in the SHE of light is generally believed as a result of an effective spin-orbital interaction, which describes the mutual influence of the spin (polarization) and trajectory of the light beam [2]. There are two characteristics of the spin-orbit interaction of photons: The first one is the influence of the trajectory upon polarization [13, 14]; The second one is the reciprocal influence of the polarization upon the trajectory [15, 16]. These mechanisms have well been understood in gradient refractive index media [13–16]. However, the physical picture in conventional beam refraction has not yet been fully examined. For example, whether the SHE can be enhanced (or suppressed) by in-

creasing (or reducing) the refractive index gradient? In addition, the relation between refractive index gradient and spin-to-orbital angular momentum conversion is also unclear. Thus, the aim of this paper is to identify the role of refractive-index gradient in the SHE of light.

The paper is organized as follows. First, we establish a relation between the refractive index gradient and polarization-dependent transverse shifts. Our result shows that the metamaterial is a viable candidate which can either amplify or eliminate the SHE of light. Under the limit of ultra-large refractive index gradient, the polarization-dependent transverse shift tends to reach a saturation value. Next, we attempt to obtain a clear physical picture of spin-to-orbital angular momentum conversion in the SHE of light. Within the paraxial approximation, a distinct separation between spin and orbital angular momenta is introduced. We find that the SHE of light may be dramatically enhanced by facilitating the spin-to-orbital angular momentum conversion. Finally, we want to explore what role refractive-index gradient plays in the spin-to-orbital angular momentum conversion. We demonstrate that the refractive index gradient can enhance or suppress the spin-to-orbital angular momentum conversion, and thus can control the SHE of light.

II. ROLE OF THE REFRACTIVE INDEX GRADIENT

To reveal the role of refractive index gradient, we need to establish a general beam propagation model for describing the SHE of light. Figure 1 illustrates the beam reflection and refraction in Cartesian coordinate system. The z axis of the laboratory Cartesian frame (x, y, z) is normal to the air-glass interface locating at $z = 0$. We use the coordinate frames (x_a, y_a, z_a) for individual beams, where $a = i, r, t$ denotes incident, reflected, and transmitted beams, respectively. In general, the electric

*Electronic address: scwen@hnu.cn

field of the a th beam can be solved by employing the Fourier transformations [17]. The complex amplitude for the a th beam can be conveniently expressed as

$$\mathbf{E}_a(x_a, y_a, z_a) = \int dk_{ax} dk_{ay} \tilde{\mathbf{E}}_a(k_{ax}, k_{ay}) \times \exp[i(k_{ax}x_a + k_{ay}y_a + k_{az}z_a)], \quad (1)$$

where $k_{az} = \sqrt{k_a^2 - (k_{ax}^2 + k_{ay}^2)}$ and $\tilde{\mathbf{E}}_a(k_{ax}, k_{ay})$ is the angular spectrum. The approximate paraxial expression for the field in Eq. (1) can be obtained by the expansion of the square root of k_{az} to the first order [18], which yields

$$\mathbf{E}_a = \exp(ik_{az}z_a) \int dk_{ax} dk_{ay} \tilde{\mathbf{E}}_a(k_{ax}, k_{ay}) \times \exp\left[i\left(k_{ax}x_a + k_{ay}y_a - \frac{k_{ax}^2 + k_{ay}^2}{2k_a}z_a\right)\right]. \quad (2)$$

Consider an incident Gaussian beam with arbitrarily polarized Gaussian beam, whose angular spectrum can be written as

$$\tilde{\mathbf{E}}_i = (\alpha \mathbf{e}_{ix} + \beta \mathbf{e}_{iy}) \exp\left[-\frac{z_R(k_{ix}^2 + k_{iy}^2)}{2k_0}\right]. \quad (3)$$

Here, $z_R = k_0 w_0^2/2$ is the Rayleigh length in free space and $k_0 = \omega/c$ is the wave number. The coefficients α and β satisfy the relation $\sigma_i = i(\alpha\beta^* - \alpha^*\beta)$. The polarization operator $\sigma_i = \pm 1$ corresponds to left and right circularly polarized light, respectively [19]. After the angular spectrum is known, we can obtain the field characteristics for the a th beam [20–23].

It is well known that the SHE of light manifests itself as polarization-dependent transverse shifts in the process of reflection and refraction. To reveal the SHE of light, we now determine the transverse shifts of beam centroid. The time-averaged linear momentum density associated with the electromagnetic field can be shown to be [24]

$$\mathbf{p}_a(\mathbf{r}) = \frac{1}{2c^2} \text{Re}[\mathbf{E}_a(\mathbf{r}) \times \mathbf{H}_a^*(\mathbf{r})], \quad (4)$$

where the magnetic field can be obtained by $\mathbf{H}_a = -ik_a^{-1} \nabla \times \mathbf{E}_a$. The intensity distribution of electromagnetic fields is closely linked to the longitudinal momentum currents $I(x_a, y_a, z_a) \propto \mathbf{p}_a \cdot \mathbf{e}_{az}$.

Figure 2 shows the transverse shifts of beam centroid in an air-glass interface. In the case of reflection, the left circularly polarized component $\sigma_i = +1$ exhibits a positive shift [Fig. 2(a)]. For the right circular polarization $\sigma_i = -1$, however, presents a positive shift [Fig. 2(b)]. In the case of transmission, the left circularly polarized component $\sigma_i = +1$ exhibits a positive transverse shift [Fig. 2(c)]. For the right circularly polarized component $\sigma_i = -1$, however, presents a negative transverse shift [Fig. 2(d)]. The transverse shifts are polarization-dependent, and thus can be regarded as the influence of

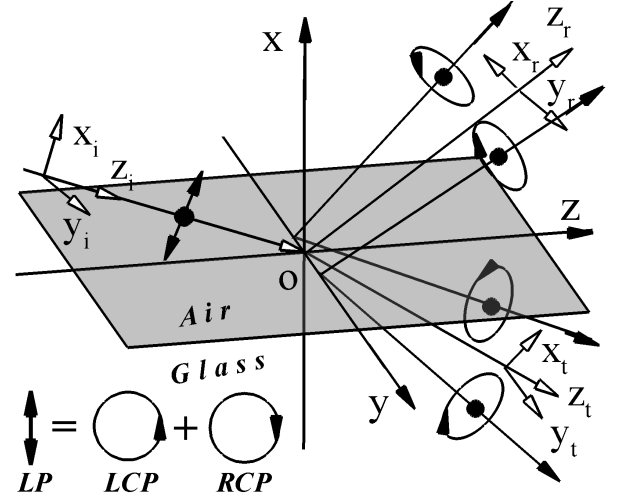


FIG. 1: Schematic illustrating the SHE of light at air-glass interface in Cartesian coordinate system. The SHE of light manifests itself as polarization-dependent transverse shifts in the process of reflection and refraction. The inset shows that the linear polarization (LP) can be regarded as a superposition of equal left circular polarization (LCP) and right circular polarization (RCP).

the polarization upon trajectory. In the air-glass interface, the transverse shifts are just a few tens of nanometers. Hence, how to amplify this tiny effect is still an open problem [1].

As we know that the refractive index gradient acts as the electric potential gradient in the electronic systems. Now a question naturally arises: Whether can the ultra-large refractive index gradient dramatically enhance the transverse shift in the SHE of light? To answer this question we need to obtain a relation between the transverse shift and the refractive index gradient. At any given plane $z_a = \text{const.}$, the transverse shift of beam centroid compared to the geometrical-optics prediction is given by

$$\langle y_a \rangle = \frac{\int \int y_a I(x_a, y_a, z_a) dx_a dy_a}{\int \int I(x_a, y_a, z_a) dx_a dy_a}. \quad (5)$$

Here, $\langle y_a \rangle$ can be written as a combination of spatial shift and angular shift: $\langle y_a \rangle = \Delta y_a + \delta y_a$. The transverse spatial shift is z_a -independent, while the transverse angular shift can be regarded as a small shift inclining from the z_a axis.

We first consider the transverse spatial shift. After substituting the reflected and the transmitted fields into Eq. (5) respectively, we have

$$\Delta y_r = -\frac{1}{k_0} \frac{f_p f_s \cot \theta_i}{|r_p|^2 f_p^2 + |r_s|^2 f_s^2} \left[(|r_p|^2 + |r_s|^2) \sin \psi + 2|r_p||r_s| \sin(\psi - \phi_p + \phi_s) \right], \quad (6)$$

$$\Delta y_t = -\frac{1}{k_0} \frac{f_p f_s \cot \theta_i}{|t_p|^2 f_p^2 + |t_s|^2 f_s^2} \left[(|t_p|^2 + |t_s|^2) \sin \psi - 2|t_p||t_s| \sin(\psi - \varphi_p + \varphi_s) \right]. \quad (7)$$

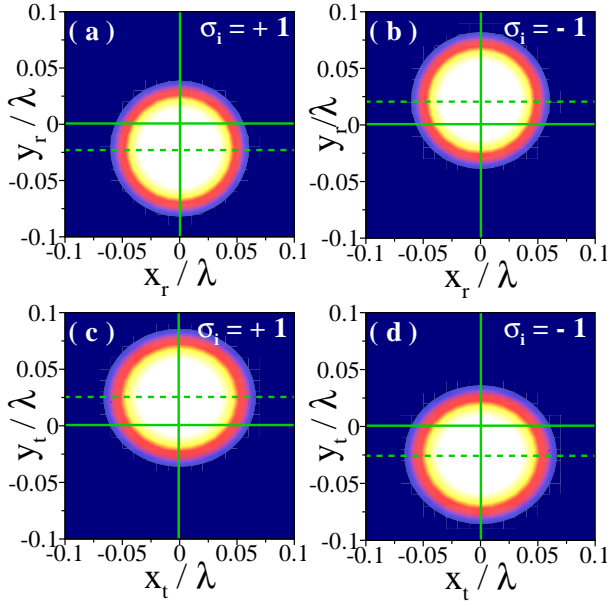


FIG. 2: (color online) The spin Hall effect manifests itself as polarization-dependent transverse shifts of field centroid. [(a), (b)] Intensity distribution of the reflected beam for $\sigma_i = +1$ and $\sigma_i = -1$ components, respectively. [(c), (d)] Intensity distribution of the transmitted beam for $\sigma_i = +1$ and $\sigma_i = -1$ components, respectively. The refractive index of the glass is $n = 1.515$ and incident angle is choose as $\theta_i = \pi/6$. The intensity distributions in the plane $z_a = 0$ are plotted in normalized units.

Here, $r_A = |r_A| \exp(i\phi_A)$ and $t_A = |t_A| \exp(i\phi_A)$ ($A = p, s$) are the Fresnel reflection and transmission coefficients, respectively. The polarization parameters $\alpha = f_p \in \text{Re}$ and $\beta = f_s \exp(i\psi)$. In the frame of classical electrodynamics, the polarization state is easily understood by observing the evolution of the electric field vector [24]:

$$\left(\frac{E_{ix}}{f_p}\right)^2 + \left(\frac{E_{iy}}{f_s}\right)^2 + 2\frac{E_{ix}E_{iy}}{f_p f_s} \cos \psi = \sin^2 \psi. \quad (8)$$

Under the limit of ultra-high refractive index gradient, the transverse spatial shifts can be written as:

$$\Delta y_r = 0, \quad (9)$$

$$\Delta y_t = -\frac{1}{k_0} \frac{f_p f_s \sin \theta_i \cos \theta_i \sin \psi}{f_p^2 + f_s^2 \cos^2 \theta_i}. \quad (10)$$

This simple result means that the ultra-high refractive index metamaterial [25] is a good candidate to eliminate the transverse spatial shift in reflected field. Otherwise, the transverse spatial shift in the transmitted field tends to reach a saturation value.

We proceed to examine the role of refractive index gradient (i.e., $\Delta n = n - 1$) in the SHE of light. Figure 3 shows the normalized transverse spatial shifts of transmitted field for various refractive index gradients.

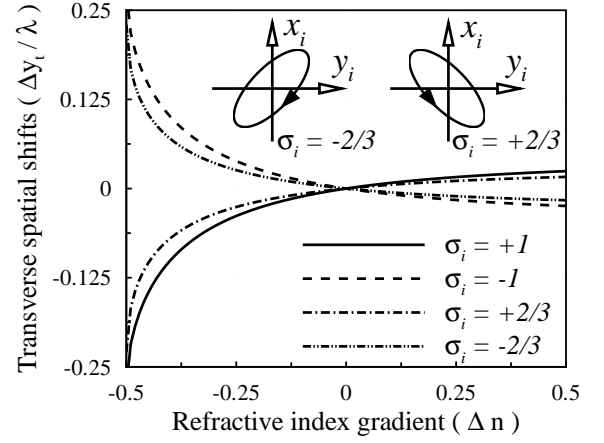


FIG. 3: The normalized transverse spatial shifts of transmitted field $\Delta y_t/\lambda$ versus refractive index gradient Δn . The polarization states of incident field are choose as $\sigma_i = +1$ (solid lines), $\sigma_i = -1$ (dashed lines), $\sigma_i = +2/3$ (dashed-dotted lines), and $\sigma_i = -2/3$ (dashed-dotted-dotted lines). Other parameters are chosen to be the same as in Fig. 2. The insets show the field structures of the two kind of elliptical polarizations.

We first consider the beam incident from air to a low-refractive-index medium ($\Delta n < 0$). For the left circularly or elliptically polarized component, the beam centroid exhibits a negative transverse shift. For the right circularly or elliptically polarized component, the beam centroid also presents a transverse spatial shift, but in an opposite direction. We next consider the beam incident from air to a high-refractive-index medium ($\Delta n > 0$). Note that the circular polarization presents a larger transverse shifts than that of the elliptical polarization. For a certain polarized component, we find that the SHE of light is reversed when the refractive index gradient is inverted. It is clearly shown that the transverse spatial shifts increases with the increase of the magnitude of the refractive index gradient $|\Delta n|$. Within the regime of low refractive index, the transverse shifts are enhanced sharply with the increase of $|\Delta n|$. While in the regime of high refractive index, the transverse shift continues increasing, then tends to reach a saturation value.

We now explore the transverse angular shifts. By substituting the reflected and the transmitted fields into Eq. (5), the transverse angular shifts are given by

$$\delta y_r = \frac{z_r}{k_0 z_R} \frac{f_p f_s (|r_p|^2 - |r_s|^2) \cot \theta_i \cos \psi}{|r_p|^2 f_p^2 + |r_s|^2 f_s^2}, \quad (11)$$

$$\delta y_t = \frac{z_t}{n k_0 z_R} \frac{f_p f_s (|t_p|^2 - |t_s|^2) \cot \theta_i \cos \psi}{|t_p|^2 f_p^2 + |t_s|^2 f_s^2}. \quad (12)$$

Note that the angle shift means that the Snell's law cannot accurately describe the beam refraction phenomenon [26]. Under the limit of ultra-high refractive index gradient, we have

$$\delta y_r = 0, \quad \delta y_t = 0. \quad (13)$$

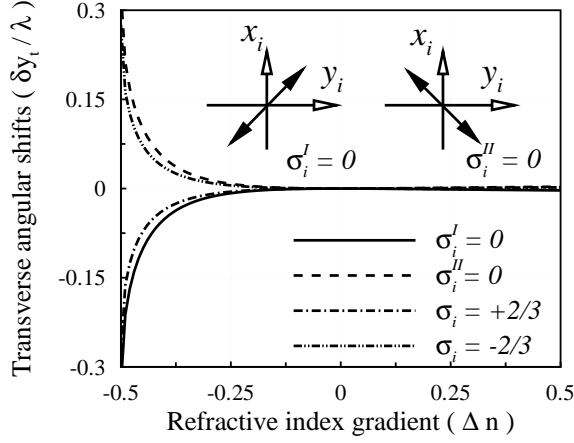


FIG. 4: The normalized transverse angular shifts $\delta y_t/\lambda$ versus the refractive index gradient Δn . Polarization parameters are chosen as $\sigma_i^I = 0$ (solid lines), $\sigma_i^{II} = 0$ (dashed lines), $\sigma_i = +2/3$ (dashed-dotted lines), and $\sigma_i = -2/3$ (dashed-dotted-dotted lines). The angular shifts are plotted in the plane $z_t = 2z_R$. Other parameters are chosen to be the same as in Fig. 2. The inset shows the polarization structure of two cases of linear polarizations.

The results clearly show that the ultra-high refractive index metamaterial is a good candidate to eliminate the angular shifts in both reflection and refraction. From Eqs. (11) and (12) we find that only special linear or elliptical polarization exhibits a transverse angular shift.

Figure 4 shows the transverse angular shifts of the transmitted field. The field structures of linear polarization are shown in the insets, and the elliptical polarization are the same as those in Fig. 3. For a left-elliptical component $\sigma_i = +2/3$ and a right-elliptical component $\sigma_i = -2/3$, the centroid of transmitted field presents an opposite angular shifts. For the two types of linear polarizations $\sigma_i^{I,II} = 0$, the centroid of transmitted field also presents opposite angular shifts. For a certain polarization, whether the transverse angular shift is positive or negative depends on the refractive index gradient. Figure 4 clearly shows that the linear polarization presents a larger transverse shift than that of the elliptical polarization. It should be noted that the transverse angular shift is significantly different from the longitudinal one [27, 28] which is polarization-independent. The transverse angular shifts are polarization-dependent, and thus can be regarded as the influence of the polarization upon the trajectory.

III. SPIN-TO-ORBITAL ANGULAR MOMENTUM CONVERSION

The spin-to-orbital angular momentum conversion can be used to explain the role of refractive index gradient in the SHE of light. To obtain a clear physical picture, we need to introduce a distinct separation between spin and orbital angular momenta. The momentum current

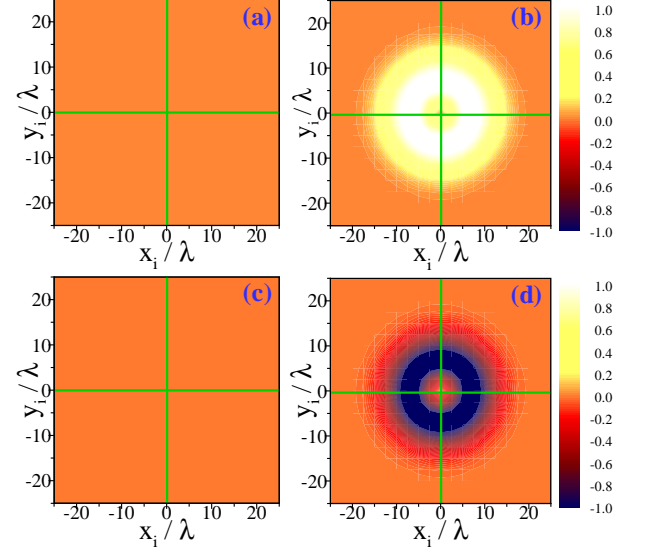


FIG. 5: (color online) The distribution of the longitudinal angular momentum density for incident beam. First row: Left circularly polarized component. Second row: Right circularly polarized component. [(a) and (c)] Orbital angular momentum density j_{iz}^O . [(b) and (d)] Spin angular momentum density j_{iz}^S . The cross section is chosen as $z_i = 0$ and the intensity is plotted in normalized units. Other parameters are the same as those in Fig. 2.

therefore can be regarded as the combined contributions of spin and orbital parts:

$$\mathbf{p}_a = \mathbf{p}_a^O + \mathbf{p}_a^S. \quad (14)$$

Here, the orbital term is determined by the macroscopic energy current with respect to an arbitrary reference point and does not depend on the polarization. The spin term, on the other hand, relates to the phase between orthogonal field components and is completely determined by the state of polarization [29]. In a monochromatic optical beam, the spin and orbital currents can be respectively written in the form:

$$\mathbf{p}_a^S = \text{Im}[(\mathbf{E}_a \cdot \nabla) \mathbf{E}_a^*], \quad (15)$$

$$\mathbf{p}_a^O = \text{Im}[\mathbf{E}_a^* \cdot (\nabla) \mathbf{E}_a], \quad (16)$$

where $\mathbf{E}_a^* \cdot (\nabla) \mathbf{E}_a = E_{ax}^* \nabla E_{ax} + E_{ay}^* \nabla E_{ay} + E_{az}^* \nabla E_{az}$ is the invariant Berry notation [30]. It has been shown that both spin and orbital currents originate from the beam transverse inhomogeneity and their components are directly related to the azimuthal and radial derivatives of the beam profile parameters. The orbital currents are mainly produced by the phase gradient, while the spin currents are orthogonal to the intensity gradient.

We proceed to analysis the angular momentum density for each of individual beam, which can be written as

$$\mathbf{j}_a(\mathbf{r}) = \mathbf{r}_a \times \mathbf{p}_a(\mathbf{r}_a). \quad (17)$$

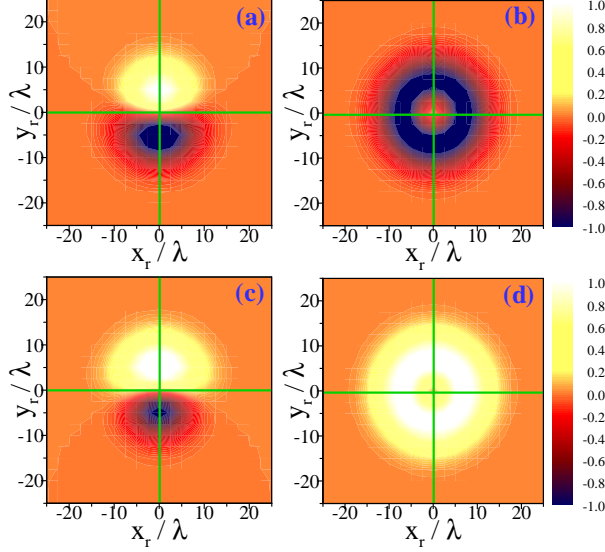


FIG. 6: (color online) The refractive index gradient induces a spin-to-orbital angular momentum conversion in reflection. First row: Left circularly polarized component. Second row: Right circularly polarized component. [(a) and (c)] Orbital angular momentum density j_{rz}^O . [(b) and (d)] Spin angular momentum density j_{rz}^S . The cross section is chosen as $z_r = 0$ and the intensity is plotted in normalized units. Other parameters are the same as those in Fig. 2.

Within the paraxial approximation, the angular momentum can be divided into the spin and orbital angular parts: $\mathbf{j}_a = \mathbf{j}_a^O + \mathbf{j}_a^S$ [31], it follows that

$$\mathbf{j}_a^O = \mathbf{r}_a \times \mathbf{p}_a^O, \quad (18)$$

$$\mathbf{j}_a^S = \mathbf{r}_a \times \mathbf{p}_a^S. \quad (19)$$

It should be mentioned that this separation still hold beyond the paraxial approximation [32]. The longitudinal angular momentum density j_z can be regarded as the combined contributions of spin and orbital parts:

$$j_{az}^O = x_a p_{ay}^O - y_a p_{ax}^O, \quad (20)$$

$$j_{az}^S = x_a p_{ay}^S - y_a p_{ax}^S. \quad (21)$$

The longitudinal angular momentum provides a simple way to understand why the beam exhibits the SHE of light.

To explore the spin-to-orbital angular momentum conversion, we consider an incident Gaussian beam with linear polarization $\sigma_i = 0$ which can be regarded as a superposition of equal left circularly polarized component $\sigma_i = +1$ and right circularly polarized component $\sigma_i = -1$. In a normal polarized model, the orbital angular momentum density is absent [Figs. 5(a) and 5(c)], and only the spin momentum density exhibits a polarization-dependent distribution [33]. For the left circular polarization, the spin angular momentum density presents a

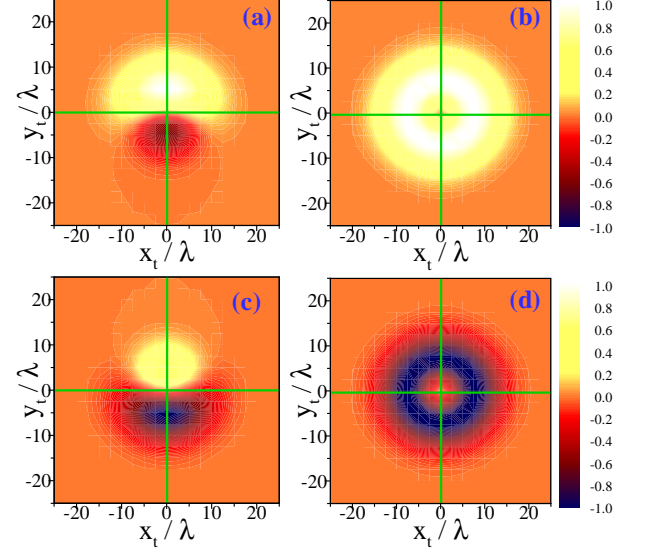


FIG. 7: (color online) The refractive index gradient induces a spin-to-orbital angular momentum conversion in the refraction. First row: Left circularly polarized beam. Second row: Right circularly polarized beam. [(a) and (c)] Orbital angular momentum density j_{tz}^O . [(b) and (d)] Spin angular momentum density j_{tz}^S . The cross section is chosen as $z_t = 0$ and the intensity is plotted in normalized units. Other parameters are the same as those in Fig. 2.

bright-ring distribution as shown in Fig. 5(b). For the right circular polarization, however, the density distribution exhibits a dark-ring as shown in Fig. 5(d). The orbital angular momentum would appear if the spin-to-orbital angular momentum conversion occurs in the process of reflection and refraction.

Figure 6 shows the spin-to-orbital angular momentum conversion in the reflection. As expected, the orbital angular momentum density exhibit a polarization-dependent distribution [Figs. 6(a) and 6(c)]. This polarization-dependent distribution of orbital angular momentum gives a direct evidence for spin-to-orbital angular momentum conversion. Compare with Fig. 5, we find that the spin angular momentum is reversed [Figs. 6(b) and 6(d)]. This interesting phenomenon seems to arise from the reversed phase of the reflection coefficient. In addition, the ring distribution of spin angular momentum density exhibits a slight aberration which is caused by the the spin-to-orbital angular momentum conversion.

We now consider the spin-to-orbital angular momentum conversion in the process of refraction. In this case, the orbital angular momentum density presents due to the spin-to-orbital angular momentum conversion [Figs. 7(a) and 7(c)]. For the left circular polarization, the spin angular momentum density exhibit a bright-ring distribution with slight aberration as shown in Fig. 7(b). For the right circular polarization, however, the spin angular momentum density presents a dark-ring distributions as shown in Fig. 7(d). The polarization-dependent

orbital angular momentum distribution is a direct reason leading to the intensity splitting in the SHE of light.

We proceed to explore the role of refractive index gradient in spin-to-orbital angular momentum conversion. The z component of total angular momentum J_{az} for the a th beam can be represented as a sum of the extrinsic orbital angular momentum J_{az}^O and the intrinsic spin angular momentum J_{az}^S , i.e., $J_{az} = J_{az}^O + J_{az}^S$ [34]. The z component of the orbital angular momenta are given by

$$J_{iz}^O = 0, \quad (22)$$

$$J_{rz}^O = -\Delta y_r k_r \sin \theta_r, \quad (23)$$

$$J_{tz}^O = -\Delta y_t k_t \sin \theta_t. \quad (24)$$

The z component of the spin angular momenta are given by $J_{iz}^S = \sigma_i \cos \theta_i$, $J_{rz}^S = \sigma_r \cos \theta_r$, and $J_{tz}^S = \sigma_t \cos \theta_t$ for incident, reflected, and transmitted beams, respectively. The spin angular momentum for the a th beam is respectively described by

$$J_{iz}^S = 2f_p f_s \sin \psi \cos \theta_i, \quad (25)$$

$$J_{rz}^S = \frac{2f_p f_s |r_p| |r_s| \sin(\psi - \phi_p + \phi_s)}{|r_p|^2 f_p^2 + |r_s|^2 f_s^2} \cos \theta_r, \quad (26)$$

$$J_{tz}^S = \frac{2f_p f_s |t_p| |t_s| \sin(\psi - \varphi_p + \varphi_s)}{|t_p|^2 f_p^2 + |t_s|^2 f_s^2} \cos \theta_t. \quad (27)$$

From Eqs. (22)-(27), we find that the angular momenta fulfill the conservation law:

$$Q_r J_{rz} + Q_t J_{tz} = J_{iz}. \quad (28)$$

Here, $Q_r = f_p^2 |r_p|^2 + f_s^2 |r_s|^2$ and $Q_t = n\eta(f_p^2 |t_p|^2 + f_s^2 |t_s|^2)$ are the energy reflection and energy transmission coefficients, respectively. In addition, the spin-to-orbital conversion can also be explained as conservation law for individual photons [35, 36].

To obtain a clear physical picture of the SHE, the spin-to-orbital angular momentum conversion is depicted in Fig. 8. For the left circularly polarized component, the spin angular momentum monotonously increase while the orbital angular momentum monotonously decreases with the increase of the refractive index gradient. For the right circular polarization, both the spin and the orbital angular momentum density present opposite features. When the refractive index gradient continues increasing, both the spin and the orbital angular momenta appear to reach saturation values:

$$J_{tz}^S = \frac{2f_p f_s \cos \theta_i \sin \psi}{f_p^2 + f_s^2 \cos^2 \theta_i}, \quad (29)$$

$$J_{tz}^O = -\frac{2f_p f_s \cos \theta_i \sin^2 \theta_i \sin \psi}{f_p^2 + f_s^2 \cos^2 \theta_i}. \quad (30)$$

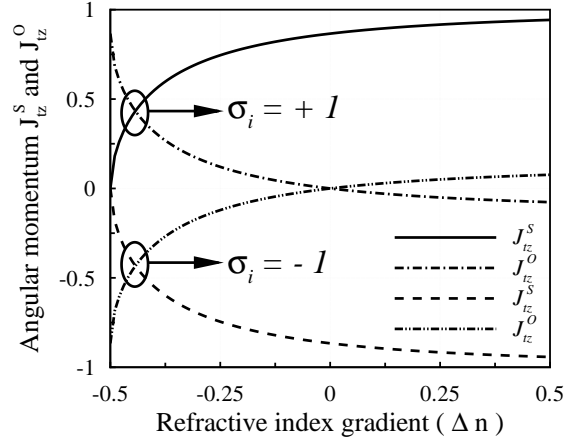


FIG. 8: The refractive index gradient induces the spin-to-orbital angular momentum conversion. Spin angular momentum (solid line) and orbital angular momentum (dashed line) for left circularly polarized component with $\sigma_i = +1$ versus refractive index gradient Δn . Spin angular momentum (dashed-dotted line) and orbital angular momentum (dash-dotted-dotted line) for right circularly polarized component with $\sigma_i = -1$ versus refractive index gradient Δn .

As the increase of the refractive index gradient, the trajectory of beam centroid experiences a deflection, which is governed by the Snell's law. Thus, this phenomenon can be regarded as the influence of the trajectory upon polarization.

We now give a very simple way to understand how the refractive index gradient enhance the spin-to-orbital angular momentum conversion in the SHE of light. We attempt to perform analyses on the z component of the total angular momentum for each of individual photons, i.e., $J_{iz} = J_{tz}$ [35]. The total angular momentum conservation law for single photon is given by

$$-\Delta y_t k_t \sin \theta_t + \sigma_t \cos \theta_t = \sigma_i \cos \theta_i. \quad (31)$$

When the photons penetrate from air into a low-refractive-index medium ($\Delta n < 0$), the incident angle is less than the transmitted angle $\theta_i < \theta_t$. For the $\sigma_i = +1$ photons, the z_t component of spin angular momentum $\sigma_t \cos \theta_t$ decreases after entering the medium. Because of the conservation law, the total angular momentum must remain unchanged. To conserve the total angular momentum, the photons must move to the direction $-y$ ($\Delta y_t < 0$) and thus generate a positive orbital angular momentum ($J_{tz}^O > 0$). For the $\sigma_i = -1$ photons, the z component of spin angular momentum $\sigma_t \cos \theta_t$ increases. In this case, the photons must move to the direction $+y$ ($\Delta y_t > 0$) and induce a negative orbital angular momentum ($J_{tz}^O < 0$). When the photons enter into a high-refractive-index medium ($\Delta n > 0$), the incident angle is larger than the transmitted angle $\theta_i > \theta_t$. As a result, the orbital angular momentum reverses its direction.

IV. CONCLUSIONS

In conclusion, we have demonstrated that the refractive index gradient can enhance or suppress the spin-to-orbital angular momentum conversion, and thus control the SHE of light. The recent advent of metamaterial whose refractive index can be tailored arbitrarily [37, 38] seems to be an available candidate to enhance the spin-to-orbital angular momentum conversion, and thus can amplify the SHE of light. However, the spin-to-orbital angular momentum conversion in a ultra-large refractive index gradient is limited by a saturation value. Fortunately, the SHE of light can be dramatically amplified by plasmonic nanostructure [39–42]. In addition, the SHE of light can also be noticeably enhanced when the beam carries orbital angular momentum [43–45]. Hence, the exploration of spin-to-orbital angular momentum conversion in these systems would be very interesting. The

transverse shifts governed by the spin-to-orbital angular momentum conversion, provide us a clear physical picture to clarify the role of refractive index gradient in the SHE of light. These findings pave a pathway for modulating the SHE of light, and thereby open the possibility for developing new nano-photonic devices. Because of the close similarity in optical physics [1, 2], condensed matter [3–5], and high-energy physics [46, 47], by properly facilitating the spin-to-orbital angular momentum conversion, the SHE may be enhanced dramatically in these physical systems.

Acknowledgments

This research was partially supported by the National Natural Science Foundation of China (Grants Nos. 10804029, 11074068, 10904036, 60890202, and 10974049).

-
- [1] O. Hosten and P. Kwiat, *Science* **319**, 787 (2008).
 - [2] K. Y. Bliokh, A. Niv, V. Kleiner, and E. Hasman, *Nature Photon.* **2**, 748 (2008).
 - [3] S. Murakami, N. Nagaosa, and S. C. Zhang, *Science* **301**, 1348 (2003).
 - [4] J. Sinova, D. Culcer, Q. Niu, N. A. Sinitsyn, T. Jungwirth, and A. H. MacDonald, *Phys. Rev. Lett.* **92**, 126603 (2004).
 - [5] J. Wunderlich, B. Kaestner, J. Sinova, and T. Jungwirth, *Phys. Rev. Lett.* **94**, 047204 (2005).
 - [6] F. I. Fedorov, *Dokl. Akad. Nauk SSSR* **105**, 465 (1955).
 - [7] C. Imbert, *Phys. Rev. D* **5**, 787 (1972).
 - [8] M. Onoda, S. Murakami, and N. Nagaosa, *Phys. Rev. Lett.* **93**, 083901 (2004).
 - [9] K. Y. Bliokh and Y. P. Bliokh, *Phys. Rev. Lett.* **96**, 073903 (2006).
 - [10] D. Haefner, S. Sukhov, and A. Dogariu, *Phys. Rev. Lett.* **102**, 123903 (2009).
 - [11] A. Aiello, N. Lindlein, C. Marquardt, and G. Leuchs, *Phys. Rev. Lett.* **103**, 100401 (2009).
 - [12] J.-M. Ménard, A. E. Mattacchione, H. M. van Driel, C. Hautmann, and M. Betz, *Phys. Rev. B* **82**, 045303 (2010).
 - [13] R. Y. Chiao and Y. S. Wu, *Phys. Rev. Lett.* **57**, 933 (1986).
 - [14] A. Tomita and R. Y. Chiao, *Phys. Rev. Lett.* **57**, 937 (1986).
 - [15] A. V. Dooghin, N. D. Kundikova, V. S. Liberman, and B. Y. Zeldovich, *Phys. Rev. A* **45**, 8204 (1992).
 - [16] V. S. Liberman and B. Y. Zeldovich, *Phys. Rev. A* **46**, 5199 (1992).
 - [17] J. W. Goodman, *Introduction to Fourier Optics* (McGraw-Hill, New York, 1996).
 - [18] M. Lax, W. H. Louisell, and W. McKnight, *Phys. Rev. A* **11**, 1365 (1975).
 - [19] R. A. Beth, *Phys. Rev.* **50**, 115 (1936).
 - [20] K. Y. Bliokh and Y. P. Bliokh, *Phys. Rev. E* **75**, 066609 (2007).
 - [21] A. Aiello and J. P. Woerdman, *Opt. Lett.* **33**, 1437 (2008).
 - [22] C. Menzel, C. Rockstuhl, T. Paul, S. Fahr, and F. Lederer, *Phys. Rev. A* **77**, 013810 (2008).
 - [23] H. Luo, S. Wen, W. Shu, Z. Tang, Y. Zou, and D. Fan, *Phys. Rev. A* **80**, 043810 (2009).
 - [24] J. D. Jackson, *Classical Electrodynamics* (Wiley, New York, 1999).
 - [25] J. Shin, J. T. Shen, and S. Fan, *Phys. Rev. Lett.* **102**, 093903 (2009).
 - [26] C. Duval, Z. Horváth, and P. A. Horváthy, *Phys. Rev. D* **74**, 021701(R) (2006).
 - [27] M. Merano, A. Aiello, M. P. van Exter, and J. P. Woerdman, *Nature Photon.* **3**, 337 (2009).
 - [28] A. Aiello, M. Merano, and J. P. Woerdman, *Phys. Rev. A* **80**, 061801(R) (2009).
 - [29] A. Y. Bekshaev and M. S. Soskin, *Opt. Commun.* **271**, 332 (2007).
 - [30] M. V. Berry, *J. Opt. A: Pure Appl. Opt.* **11**, 094001 (2009).
 - [31] L. Allen, M. W. Beijersbergen, R. J. C. Spreeuw, and J. P. Woerdman, *Phys. Rev. A* **45**, 8185 (1992).
 - [32] S. M. Barnett, *J. Opt. B* **4**, S7 (2002).
 - [33] H. Luo, S. Wen, W. Shu, and D. Fan, *Phys. Rev. A* **81**, 053826 (2010).
 - [34] K. Y. Bliokh, I. V. Shadrivov, and Y. S. Kivshar, *Opt. Lett.* **34**, 389 (2009).
 - [35] M. Onoda, S. Murakami, and N. Nagaosa, *Phys. Rev. E* **74**, 066610 (2006).
 - [36] W. Nasalski, *Phys. Rev. E* **74**, 056613 (2006).
 - [37] D. R. Smith, J. B. Pendry, and M. C. K. Wiltshire, *Science* **305**, 788 (2004).
 - [38] J. Pendry, D. Schurig, and D. Smith, *Science* **312**, 1780 (2006).
 - [39] Y. Gorodetski, A. Niv, V. Kleiner, and E. Hasman, *Phys. Rev. Lett.* **101**, 043903 (2008).
 - [40] Y. Gorodetski, N. Shitrit, I. Bretner, V. Kleiner, and E. Hasman, *Nano Lett.* **9**, 3016 (2009).
 - [41] L. T. Vuong, A. J. L. Adam, J. M. Brok, P. C. M. Planken, and H. P. Urbach, *Phys. Rev. Lett.* **104**, 083903 (2010).
 - [42] O. G. Rodríguez-Herrera, D. Lara, K. Y. Bliokh, E. A. Ostrovskaya, and C. Dainty, *Phys. Rev. Lett.* **104**, 253601 (2010).

- [43] K. Y. Bliokh, Phys. Rev. Lett. **97**, 043901 (2006).
- [44] T. A. Fadeyeva, A. F. Rubass, and A. V. Volyar, Phys. Rev. A **79**, 053815 (2009).
- [45] M. Merano, N. Hermosa, J. P. Woerdman, and A. Aiello, Phys. Rev. A **82**, 023817 (2010).
- [46] A. Bérard and H. Mohrbach, Phys. Lett. A **352**, 190 (2006).
- [47] P. Gosselin, A. Bérard, and H. Mohrbach, Phys. Rev. D **75**, 084035 (2007).